Lorenz type attractor in electronic parametric generator and its transformation outside the parametric resonance

S.P. Kuznetsov

Kotel'nikov's Institute of Radio-Engineering and Electronics of RAS, Saratov Branch, Zelenaya 38, Saratov 410019, Russia

e-mail: spkuz@yandex.ru

For parametric generator composed of three LC-circuits and quadratic nonlinear element on the basis of the operational amplifier and analog multiplier the equations for the interacting mode amplitudes are derived. At frequencies providing the parametric resonance precisely, the problem reduces to a system of three differential-equations of the first order for the amplitudes with attractor of Lorenz type. In the presence of the detuning ot only to the dynamics of the amplitude is relevant, but also the phase dynamics. Attractor must be considered now in the six-dimensional phase space, and in contrast to the Lorenz attractor it is not quasi-hyperbolic.

Keywords: parametric oscillator, the Lorenz attractor, analog simulation

Introduction

This chapter is inspired by seminal works of M.I. Rabinovich and his collaborators in 70-th devoted to complex dynamics of parametric oscillators [1,2,3], mainly, by the article of Pikovsky, Rabinovich and Trakhtengerts [2]. It was shown there that in a case of parametric excitation of two modes by means of the pump at the sum frequency and the energy transfer to decaying third mode at the difference frequency chaotic dynamics can occur. Particularly, the authors of [2] considered the situation in application to waves in magnetized plasma. Assuming a quadratic nonlinearity, they formulated a system of amplitude equations, which in the case of a fixed phase relation was reduced to a system of three differential equations of the first order possessing the Lorenz type attractor. The same mechanism of chaos generation can be implemented with the parametric interaction of waves or oscillatory modes in various physical objects, such as mechanical, electronic, optical, acoustic systems [4-7].

Lorenz attractor is a popular example of a strange chaotic attractor [8-10], which was originally discovered in a model system of three first order differential equations for the problem of fluid convection in a layer heated from below. It belongs to a class of singular hyperbolic (quasi-hyperbolic) attractors [11,12] and generates robust chaos [13,14] in the sense that the chaotic behavior is not destroyed by a small variation of the system parameters. In the years after the Lorenz publication it became clear that this type of attractor may be related to many different natural systems, including laser dynamics [15-16], mechanical systems based on the rigid body rotations [18-21] and others [22 -26].

Some aspects of the dynamics of the model of Pikovsky, Rabinovich and Trakhtengerts were analyzed later by other authors. In particular, it concerns the dynamics, accompanied by violation of the phase locking [30], comparison of the model with a 10-dimensional system for the problem of the interaction of waves in plasma [31], and mathematical analysis of global dynamics [32]. In [33] an electronic parametric oscillator was considered based on three resonant LC circuits, the operation of which is provided by the decay mechanism of the instability saturation, where the parametric excitation and the interaction of modes take place due to the presence of a varactor diode. It has been found that with accurate description of the nonlinear characteristic of the diode, the equations for slow amplitudes are essentially represented in complex variables, so that in the dynamics of the excited oscillatory modes the phases are relevant, and the attractor ceases to be quasi-hyperbolic. In particular, this is expressed by appearance of domains of regularity in the parameter space, where the periodic dynamics occur instead of chaos, and attractors are represented by limit cycles.

In this presentation we analyze the parametric oscillator circuit similar to that in Ref. [33], but using a specially designed reactive nonlinear element composed on a basis of an operational amplifier and an analog multiplier, with the characteristic exactly given by a quadratic function. Because of this it is possible to realize the pure dynamics of the Pikovsky – Rabinovich – Trakhtengerts model in pure form; with exact parametric resonance conditions it manifests the Lorenz type attractor. In the case of violation of the exact frequency relations a situation occurs similar to that observed in Ref. [33]. Namely, the phase dynamics becomes relevant; the attractor ceases to be quasi-hyperbolic, and domains of regular dynamics appear in the parameter space besides the chaos.

1. Parametric oscillator circuit diagram and the basic equations

Consider the circuit diagram of Figure 1a. It is composed of three resonant circuits L_1-C_1, L_2-C_2 and L_3-C_3. Parametric excitation is provided by the pump from the AC voltage source V_1 in presence of the quadratic nonlinear reactive element $\widetilde{C}$.
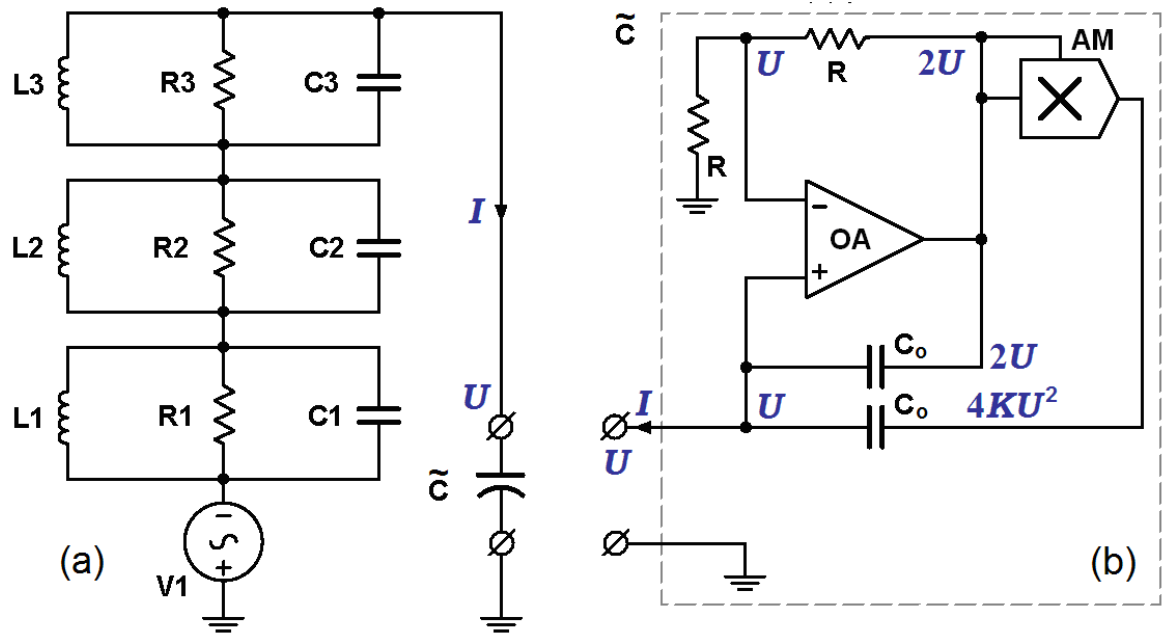

Figure 1: The circuit diagram of the chaotic parametric oscillator (a). The pumping is provided by the voltage source V_1. The symbol $\widetilde{C}$ denotes a reactive two-pole element with quadratic nonlinearity, the scheme of which is shown separately on the panel (b).

The nonlinear element circuit diagram is shown separately in panel (b). When a voltage U is applied to the input of the element with respect to the ground, the potential U takes place on the both input terminals of the operational amplifier OA. Since the input impedance of the operational amplifier ideally is infinite, the presence of the current U/R through the resistor R, which has a grounded outlet, implies the presence of the same current through the second resistor R connected to the previous one, and thus the voltage at the input of the analog multiplier AM must be equal to $2U$. Hence we have the voltage $4KU^2$ at its output. The currents through the one and the other capacitors C_0 are $C_0 \dfrac{dU}{dt}$ and $\dfrac{d}{dt}\left(4KU^2 - C_0 U\right)$ comprise, in an amount, the current $\dfrac{d}{dt}\left(4KU^2\right)$ through the nonlinear element.

The natural frequencies of the LC resonant circuits (without taking into account the dissipation) will be assumed to satisfy, at least approximately, the parametric resonance conditions

$$\Omega_0 \approx \Omega_1 + \Omega_2, \ \Omega_3 \approx \Omega_1 - \Omega_2 . \tag{1}$$

2

Figure 2 shows plots of voltages on the capacitors C1, C2 and C3 obtained from the virtual oscilloscope in the course of simulation using the Multisim environment of the circuit with the component values indicated in the figure caption. After the transient decay, a sustained regime of nonlinear oscillations persists. In the scale of the figure, the high-frequency filling is indistinguishable, but one can observe clearly the irregular, apparently chaotic behavior of the amplitudes.
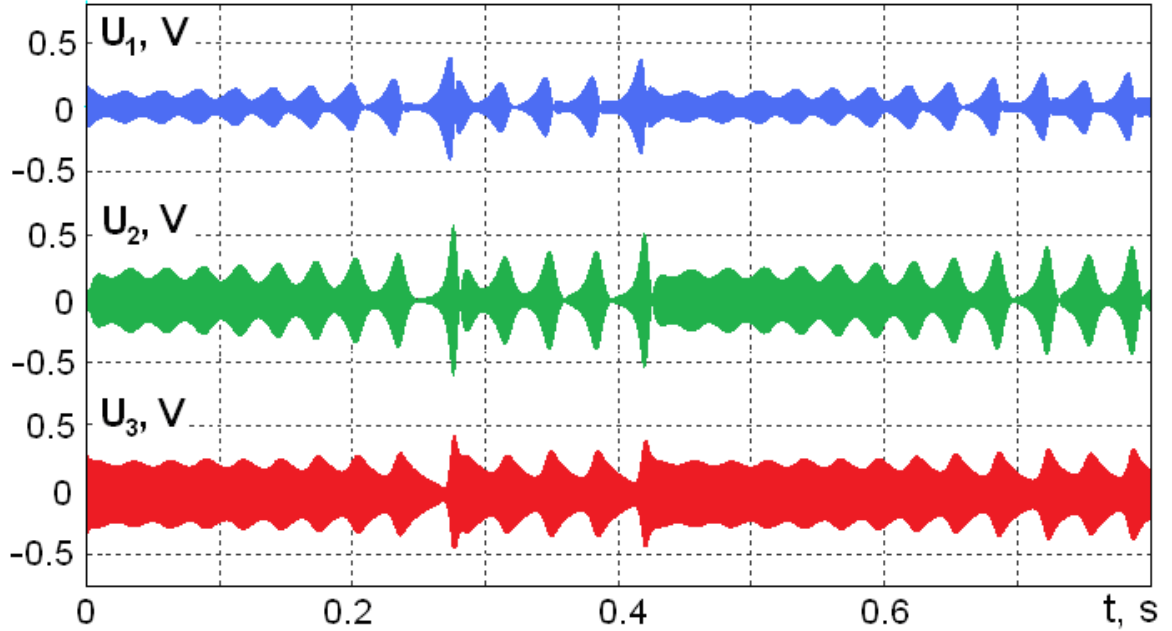

Figure 2: Typical waveforms for the voltages across the capacitors C_1, C_2, C_3 obtained by simulation of the circuit of Figure 1 using the Multisim environment. The component values: $C_1=C_2=C_3=40$ nF, $L_1=1.583$ mH, $L_2=4.398$ mH, $L_3=9.895$ mH, $R_1=250$ kΩ, $R_2=62.5$ kΩ, $R_3=250$ kΩ. The natural frequencies of the LC circuits are $f_1=20$ kHz, $f_2=12$ kHz, $f_3=8$ kHz. Pumping is carried out by the voltage source V_1 with amplitude of 0.245 V at the frequency $f_0=32$ kHz. The capacitors in the circuit diagram of the nonlinear reactive element are of capacitance $C_0 = 2$ nF; the transmission coefficient of the analog multiplier AM is K = 1/8 V^{-1}.

In a framework of the circuit simulation in Multisim it is difficult to get information concerning some of essential features of the dynamics including the expected presence of the Lorenz type attractor and to determine relevant characteristics such as the Lyapunov exponents. Therefore, in the following sections we will discuss the equations describing the system, and analyze some results of their numerical integration.

2. Basic equations of the parametric oscillator

Suppose that U_1, U_2, U_3 are voltages on the capacitors C1, C2, C3, and I_1, I_2, I_3 are currents through the inductors L1, L2, L3. Assuming equality of the capacities $C = C_1 = C_2 = C_3$ for simplicity, write down the Kirchhoff equations as follows:

$$
\begin{aligned}
L_1 \dot{I}_1 &= U_1, \\
L_2 \dot{I}_2 &= U_2, \\
L_3 \dot{I}_3 &= U_3, \\
C\dot{U}_1 + U_1 / R_1 + I_1 &= -I, \\
C\dot{U}_2 + U_2 / R_2 + I_2 &= -I, \\
C\dot{U}_3 + U_3 / R_3 + I_3 &= -I.
\end{aligned}
\tag{2}
$$

Here *I* is the current through the non-linear element defined by the expression

3

$$I = \frac{d}{dt}4KC_0U^2 = C\varepsilon\frac{d}{dt}\frac{U^2}{2},\tag{3}$$

where

$$\varepsilon = 8KC_0 / C, \ U = U_1 + U_2 + U_3 + U_0, \ U_0 = -\kappa\sin\omega_0 t,\tag{4}$$

and the values of κ and ω_0 designate the amplitude and frequency of the pump signal. Using the normalized dimensionless time $t' = t /(2R_3C)$, the equation can be rewritten as

$$\ddot{X}_k + 2\nu_k\dot{U}_k + \Omega_k^2 U_k = 0, \ X_k = U_k + \tfrac{1}{2}\varepsilon U^2, \ k = 1,2,3,\tag{5}$$

where

$$\nu_{1,2} = \frac{R_3}{R_{1,2}}, \ \nu_3 = 1, \ \Omega_{1,2,3} = 2R_3\sqrt{\frac{C}{L_{1,2,3}}}.\tag{6}$$
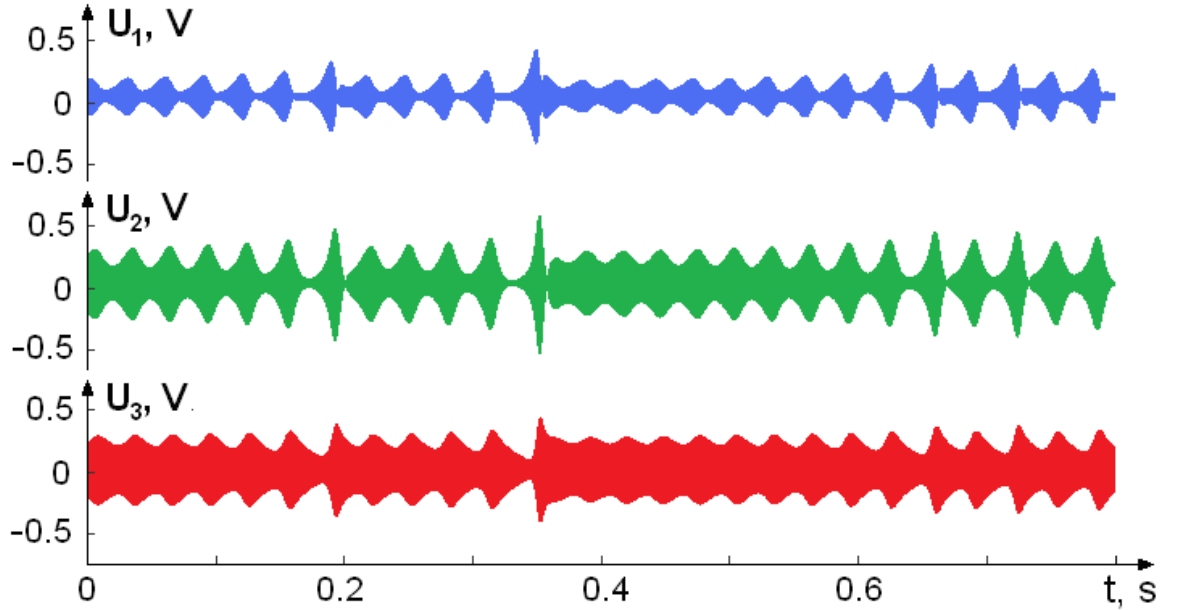

Figure 3: Typical waveforms of voltages across the capacitors C_1, C_2, C_3, obtained from numerical integration of the equations (7) for the circuit shown in Figure 1, with component values indicated in the caption of Figure 2.

For the numerical integration it is convenient to reformulate the problem representing it by the set of the first order differential equations

$$\dot{Y}_k = -\Omega_k(X_k - \tfrac{1}{2}\varepsilon U^2), \quad \dot{X}_k = \Omega_k Y_k - 2\nu_k, \quad k = 1, 2, 3,$$
$$U = \frac{-1 + \sqrt{6\varepsilon(X_1 + X_2 + X_3 - \kappa\sin\Omega_0 t') + 1}}{3\varepsilon}, \ U_i = X_k - \tfrac{1}{2}\varepsilon U^2.\tag{7}$$

Figure 3 shows the time dependences for the quantities U_1, U_2, U_3, obtained by numerical integration of the equations (7) with component values indicated in the caption to Figure 2 values. Comparing the plots in Figure 2 and 3, we can see a good agreement between the observed dynamics. In both cases we have chaotic waveforms containing similar fragments, and compliance in characteristic scales of times and voltages. (One should not expect to see exact correspondence of the waveforms because of the inherent sensitivity of the chaotic dynamics to small perturbations of the initial conditions.)

3. Equations for slow amplitudes

To obtain equations in a form that allows comparison with the Lorenz and Pikovsky – Rabinovich – Trakhtengerts models, it is necessary to apply the method of slow complex amplitudes. First, it is convenient to rewrite the equation considering only those terms,

4

which can contribute to the resonant interaction of the modes corresponding to the relation of the frequencies (1). In the first, the second and the third equations (5) one can set, respectively,

$$\frac{1}{2}U^2 \approx U_0 U_2 + U_2 U_3,$$
$$\frac{1}{2}U^2 \approx U_0 U_1 + U_1 U_3,$$
$$\frac{1}{2}U^2 \approx U_1 U_2.$$

(8)

In addition, replace the operation of the second derivative of the nonlinear terms in the the equations by the multiplier $(-\Omega_k^2)$. The result is

$$\ddot{U}_1 + 2\nu_1 \dot{U}_1 + \Omega_1^2 U_1 = \varepsilon \Omega_1^2 (U_0 U_2 + U_2 U_3),$$
$$\ddot{U}_2 + 2\nu_2 \dot{U}_2 + \Omega_2^2 U_2 = \varepsilon \Omega_2^2 (U_0 U_1 + U_1 U_3),$$
$$\ddot{U}_3 + 2\dot{U}_3 + \Omega_3^2 U_3 = \varepsilon \Omega_3^2 U_1 U_2.$$

(9)

Omitting for brevity the prime at the time variable, we seek a solution in the form

$$U_1 = A_1 e^{i\omega_1 t} + A_1^* e^{-i\omega_1 t}, \quad \dot{U}_1 = i\omega_1 A_1 e^{i\omega_1 t} - i\omega_1 A_1^* e^{-i\omega_1 t},$$
$$U_2 = A_2 e^{i\omega_2 t} + A_2^* e^{-i\omega_2 t}, \quad \dot{U}_2 = i\omega_2 A_2 e^{i\omega_2 t} - i\omega_2 A_2^* e^{-i\omega_2 t},$$
$$U_3 = -iA_3 e^{i\omega_3 t} + iA_3^* e^{-i\omega_3 t}, \quad \dot{U}_3 = \omega_3 A_3 e^{i\omega_3 t} + \omega_3 A_3^* e^{-i\omega_3 t},$$

(10)

where the reference frequencies $\omega_{1,2,3}$ are defined as

$$\omega_1 = \frac{\Omega_1 - \Omega_2 + \Omega_0}{2}, \quad \omega_2 = \frac{-\Omega_1 + \Omega_2 + \Omega_0}{2}, \quad \omega_3 = \Omega_1 - \Omega_2.$$

(11)

Been close to the values $\Omega_{1,2,3}$ they satisfy the parametric resonance conditions precisely:

$$\omega_3 = \omega_1 - \omega_2, \quad \Omega_0 = \omega_1 + \omega_2.$$

(12)

Use of (10) implies fulfillment of the additional equalities for the amplitude variables

$$\dot{A}_1 e^{i\omega_1 t} + \dot{A}_1^* e^{-i\omega_1 t} = 0, \quad \dot{A}_2 e^{i\omega_2 t} + \dot{A}_2^* e^{-i\omega_2 t} = 0, \quad \dot{A}_3 e^{i\omega_3 t} - \dot{A}_3^* e^{-i\omega_3 t} = 0.$$

(13)

Next, according to (4), we have

$$U_0 = -\kappa \sin \Omega_0 t = \frac{1}{2} i\kappa e^{i\Omega_0 t} - \frac{1}{2} i\kappa e^{-i\Omega_0 t}.$$

(14)

Substitution of (10) into Eqs. (9) yields

$$\dot{A}_1 + \nu_1 A_1 - i\Delta A_1 = \frac{1}{2}\varepsilon\Omega_1(\frac{1}{2}\kappa A_2^* - A_2 A_3),$$
$$\dot{A}_2 + \nu_2 A_2 - i\Delta A_2 = \frac{1}{2}\varepsilon\Omega_2(\frac{1}{2}\kappa A_1^* + A_1 A_3^*),$$
$$\dot{A}_3 + A_3 - i\delta A_3 = \frac{1}{2}\varepsilon\Omega_3 A_1 A_2^*,$$

(15)

where

$$\Delta \approx \Omega_1 - \omega_1 = \Omega_2 - \omega_2 = \frac{\Omega_1 + \Omega_2 - \Omega_0}{2}, \quad \delta \approx \Omega_3 - \omega_3 = \Omega_3 - \Omega_1 + \Omega_2.$$

With normalization

$$A_1 = \frac{2}{\varepsilon\sqrt{\Omega_2 \Omega_3}} a_1, \quad A_2 = \frac{2}{\varepsilon\sqrt{\Omega_3 \Omega_1}} a_2, \quad A_3 = \frac{2}{\varepsilon\sqrt{\Omega_1 \Omega_2}} a_3, \quad h = \frac{\varepsilon\kappa\sqrt{\Omega_1 \Omega_2}}{4},$$

(16)

we obtain the equations exactly corresponding to Ref. [2]:

$$\dot{a}_1 + \nu_1 a_1 - i\Delta a_1 = ha_2^* - a_2 a_3, \quad \dot{a}_2 + \nu_2 a_2 - i\Delta a_2 = ha_1^* + a_1 a_3^*, \quad \dot{a}_3 + a_3 - i\delta a_3 = a_1 a_2^*.$$

(17)

Here κ is the dimensionless parameter of the amplitude of pumping. The value Δ can be adjusted by varying the pumping frequency and the δ by varying the inductance L_3.

4. Precise parametric resonance: Lorenz type attractor

In the absence of detuning, $\Delta=0$, $\delta=0$, using the substitution

$$a_1 = xe^{i\varphi}, \ a_2 = ye^{-i\varphi}, \ a_3 = ze^{2i\varphi} \tag{18}$$

with $\varphi = \text{const}$ we arrive at the equations

$$\dot{x} = hy - v_1 x - yz, \ \dot{y} = hx - v_2 y + xz, \ \dot{z} = -z + xy, \tag{19}$$

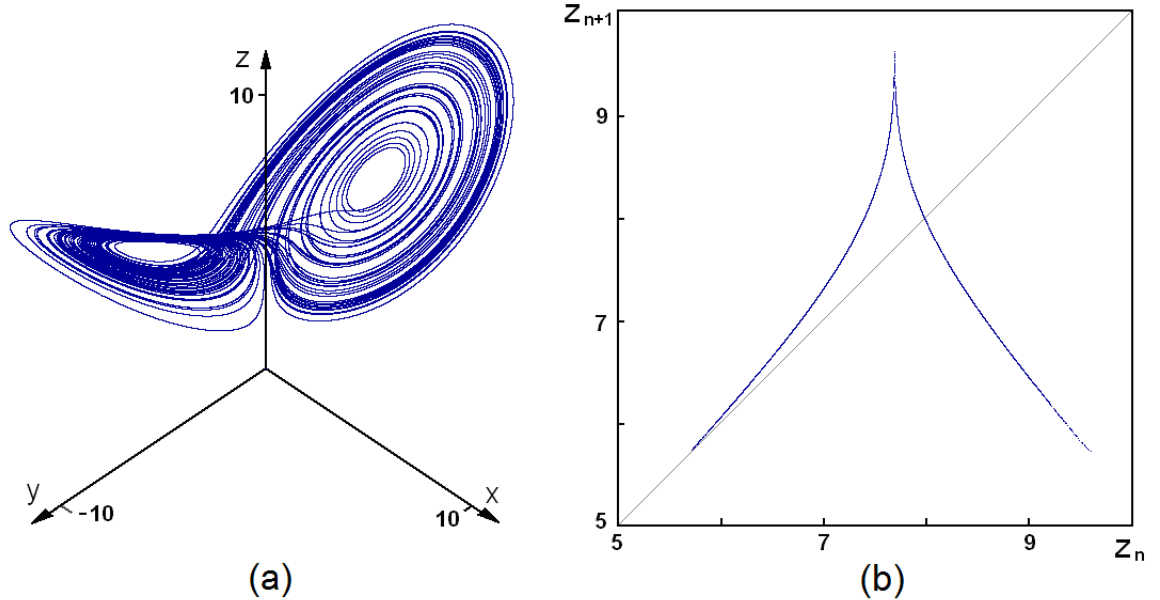which may be considered in the real domain.

(a) (b)

Figure 4: Attractor in the three-dimensional state space of the system (19) (a) and plot of the map for successive maxima of the variable z in the course of temporal evolution (b); parameters are $v_1 = 1$, $v_2 = 4$, $h = 5.962$.

According to [2], the model (19) has attractor of Lorenz type in the three-dimensional phase space of the variables x, y, z, which is true, particularly, in the case $v_1 = 1$, $v_2 = 4$, $h = 5.962$. Figure 4 shows a portrait of the attractor, depicted with the results of numerical integration of the equations (19). Also, the plot is shown obtained in accordance with the procedure applied by Lorenz in his work [8]: on the axes are the values of the maxima of the variable z achieved sequentially during the time evolution of the system. The view of the plot with a sharp peak, which resembles a classic "saw tooth" map [8-10,2], indicates that the attractor is quasi-hyperbolic, just like the classic Lorenz attractor.

The Lyapunov exponents calculation by joint numerical solution of equations (19) and the corresponding variational equations is based on a known algorithm with Gram - Schmidt orthogonalization perturbation vectors [37, 10] and yields [1]

$$\lambda_1 = 0.394 \pm 0.001, \ \lambda_2 = 0.0000 \pm 0.0001, \ \lambda_3 = -6.394 \pm 0.001. \tag{20}$$

The presence of a positive Lyapunov exponent indicates occurrence of chaos, characterized by the exponential growth of the deviation from the reference trajectory on the attractor under small perturbations of the initial conditions. The second exponent is zero up to a calculation error; it is associated with a perturbation of a shift along the phase trajectory. The third exponent is negative and is responsible for the approach of the trajectories to the attractor. The fact that the sum of the exponents is negative indicates the volume compression in the three-dimensional phase space. It is consistent with the

---

[1] Lyapunov exponents' calculations were performed on time intervals of duration of 50,000 with the counting the average values and standard deviations on 20 samples. As an error, the standard deviations are indicated.

analytical calculation of the divergence of the vector field defined by the right sides of the equations (19): $\mathrm{div}\mathbf{F} = \partial_x f_x + \partial_y f_y + \partial_z f_z = -\nu_1 - \nu_2 - 1 = -6$. Estimate of the dimension of the attractor for the well-known formula of Kaplan – Yorke provides $D = 2 + \lambda_1 / |\lambda_3| \approx 2.06$.

Figure 5 shows the three Lyapunov exponents of the model (19) versus the parameter h. The smooth nature of the dependence and the lack of notable dips (regularity windows) for the senior exponent in the graph indicate the robustness of chaos in the three-dimensional system (19) and correspond to the conclusion that the nature of the attractor is quasi-hyperbolic as motivated by the view of the graph displayed on Figure 4b.

It is interesting to compare the Lyapunov exponents calculated at the same parameters for equations in real and complex amplitudes. For the system (17) at $\Delta=0$, $\delta=0$ we have

$$\lambda_1 = 0.394 \pm 0.001, \ \lambda_2 = 0.0000 \pm 0.0002, \ \lambda_3 = 0.0000 \pm 0.0003,$$
$$\lambda_4 = -0.618 \pm 0.05, \ \lambda_5 = -5.381 \pm 0.05, \quad \lambda_6 = -6.394 \pm 0.003. \tag{21}$$

In this list, there are two zero exponents, one of which is associated with the shift perturbation along the phase trajectory, the second with the phase shifted in the variable φ (see (18)). The exponents $\lambda_{1,2,6}$ are in agreement with the exponents $\lambda_{1,2,3}$ from the list (20). Additional exponents $\lambda_{4,5}$ correspond obviously to the relaxation of phases to the situation described by equations for real amplitudes. Figure 5 shows the dependence on h for six Lyapunov exponents of the model (17), three of which are indistinguishable from those of the model (19).
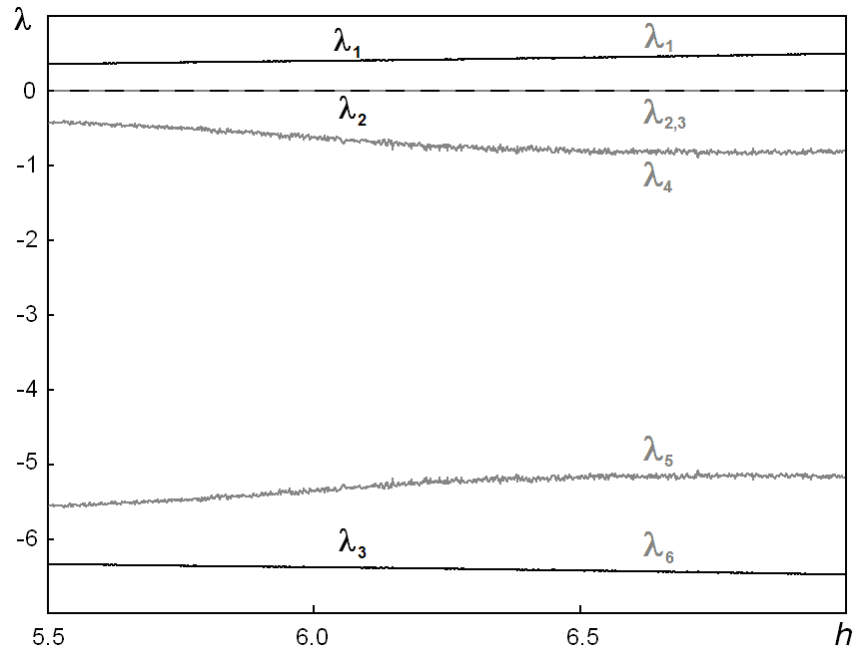

Figure 5: The dependence on the parameter h for the Lyapunov exponents. The exponents of the model (19) are marked as λ_{1-3} on the left side of the diagram, and those for the model (17) at $\Delta=0$, $\delta=0$ are labeled as λ_{1-6} in the right part of the figure. Other parameters: $\nu_1 = 1$, $\nu_2 = 4$.

If we talk about the system without reduction to the slow amplitudes (7) and a about the model with complex amplitudes (17), it would be incorrect to relate to them the conclusion concerning robustness of the Lorenz type attractor from the three-dimensional real model (19). A formal sign pointing to a possible violation of the robustness in this sense is the occurrence of the additional zero Lyapunov exponent in the complex system (17). In particular, introduction of the frequency detuning leads to a disruption of the phase relations (18) and to a change in the nature of the attractor.

5. Chaotic and regular dynamics in the parametric oscillator in presence of frequency detuning

We now turn to the situation when the conditions of parametric resonance are not accurately fulfilled, and one has to take into account the frequency detuning of the pump from the sum of natural frequencies of the first and second oscillators, and detuning of the difference frequency from the frequency of the third oscillator. This corresponds to non-zero parameters Δ, δ in the complex amplitude equations (17), which can not reduced now to the three-dimensional system for real amplitudes.

In this situation, there is a problem of graphical presentation of attractors in the form allowing a visual comparison with the Lorenz attractor. We proceed from the fact that the approximate correspondence of instantaneous phase of the complex variables a_1 and a_2 to the formulas (18) roughly persists for the most part, although the value of φ, generally speaking, will not be constant in time. For graphical representation it is natural to use the variables $x = \operatorname{Re} a_1 e^{-i\varphi}$, $y = \operatorname{Re} a_2 e^{i\varphi}$, where φ is chosen each time to minimize the value $(\operatorname{Im} a_1 e^{-i\varphi})^2 + (\operatorname{Im} a_2 e^{i\varphi})^2$. As the third variable we use $z = |a_3|$.

Note that the same method can be used for processing data of the numerical solution of the original Kirchhoff equations (7) if convert the vectors defined by the voltages $\mathbf{U} = (U_1, U_2, U_3)^{\mathrm{T}}$, to the complex amplitudes as

$$a_{1,2,3} = \tfrac{1}{2}(U_{1,2,3} - i\omega_{1,2,3}^{-1}\dot{U}_{1,2,3}).\qquad(22)$$

Figure 6a shows a portrait of the attractor, built with the results of the numerical integration of equations (17) in a mode corresponding to a slight shift of the pump frequency from the exact parametric resonance conditions at $h = 5.962$, $\nu_1 = 1$, $\nu_2 = 4$, $\Delta = 0.3$, $\delta = 0$. (In the original system, this corresponds to the pumping frequency of 32001.2 Hz at amplitude of 62.25 mV setting resistances $R_1 = 1$ MΩ, $R_2 = 250$ kΩ, $R_3 = 1$ MΩ and the remaining components correspond to the caption of Figure 2.) The phase portrait looks like Lorenz type attractor: it has two "wings", each of which corresponds to orbit spiraling from the central blank area, with successive transitions from one wing to the other, and the committed numbers of turns vary from once again chaotically.

Figure 6b shows a plot of the map, where the axes correspond to successive maxima of the variable $z = |A_3|$ achieved in the course of the temporal evolution of the system. The picture is significantly different from the map corresponding to the Lorenz type attractor in Figure 4. Firstly, the graph looks composed not of a single curve, but a set of curves, i.e. it possesses a transverse fractal structure expressed much stronger than that for the Lorenz type attractor, where it is visually indistinguishable. Secondly, the curves representing the mapping manifest smooth quadratic maxima instead of a sharp tip at the top. In this connection, in this case one can not speak of robust quasi-hyperbolic attractor. Rather, the properties of chaotic dynamics should be similar to attractors in the Hénon map [38] and Rössler model [39], which in mathematical works are interpreted within the concept of quasi-attractor [40,41].

Figure 7 shows the dependence of six Lyapunov exponents of the model (17) on parameters of the frequency detuning Δ and δ. Note the symmetry of one and the other graph in Figure 7; it occurs due to the fact that the equations transform into themselves in the application of the complex conjugation together with the sign change of Δ and δ.

Unlike the case of exact resonance, the graph for the senior Lyapunov exponent manifests dips (the regularity windows), which are also accompanied by tips or dips in the graphs of other exponents. As one can verify by the numerical integration of the equations, these windows correspond to the emergence of attracting limit cycles in the phase space of the system (17), i.e., instead of chaos modes periodic oscillations of the amplitude variables arise. It is this kind of the plots for Lyapunov exponents depending on a parameter which is intrinsic particularly for one-dimensional maps with quadratic

extremum and for many other dissipative systems, including the Hénon map and the Rössler model, which are associated with the concept of quasi-attractor [38-41].
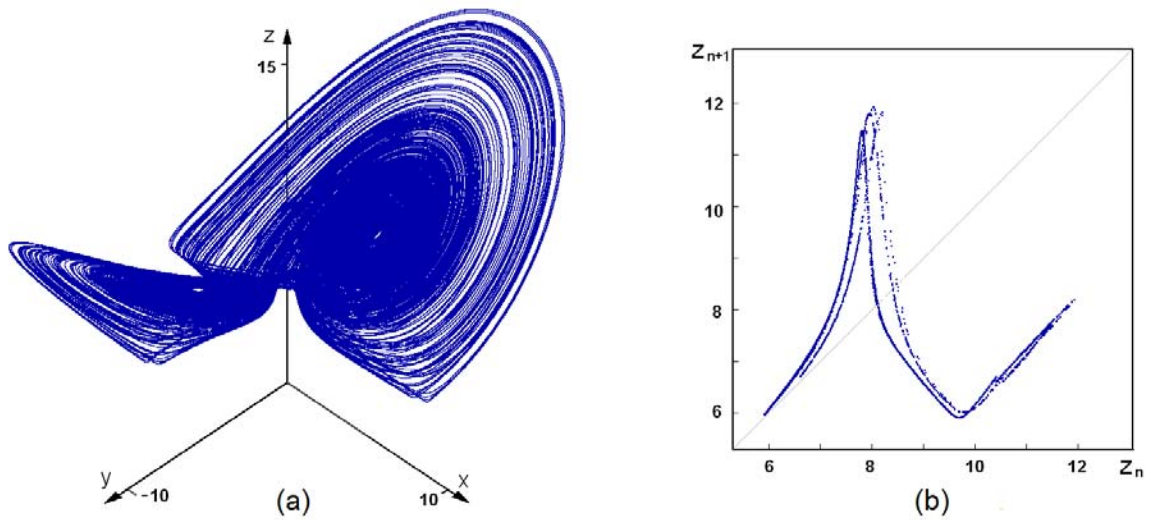

Figure 6: Three-dimensional portrait of the attractor, built using the techniques described in the text (a), and a plot of the map for successive maxima of the variable $z = |a_3|$ (b) for the system (17) at $h = 5.962$, $\nu_1 = 1$, $\nu_2 = 4$, $\Delta = 0.3$, $\delta = 0$.
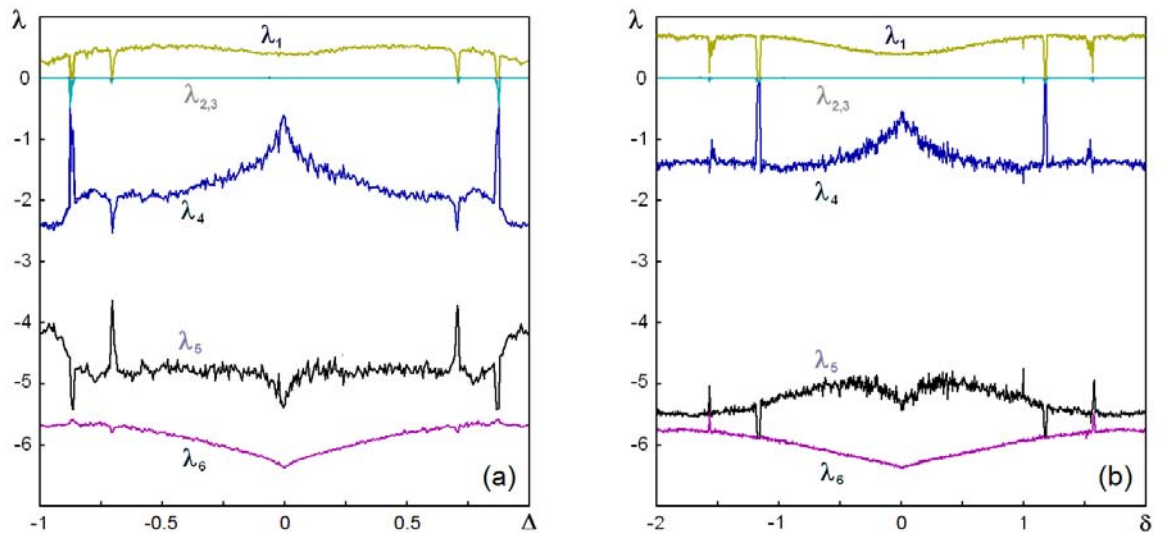

Figure 7: Lyapunov exponents of the model (17) versus parameter Δ at $\delta = 0$ (a) and versus parameter δ at $\Delta = 0$ (b). Other parameters: $\nu_1 = 1$, $\nu_2 = 4$.

Let us turn to the chart of dynamical regimes in the parameter plane Δ, δ. The procedure consists of scanning of a parameter space area in two dimensions over the grid nodes with some small step. At each point about 10^3 iterations of the Poincaré map is performed defined for the system (17) via the section surface $S = |a_3| - h + \sqrt{\nu_1 \nu_2} = 0$ in the phase space (in the direction of passage of the orbits with decreasing S). According to the latest iterations the analysis is carried out for the presence or absence of a repetition period of the states in the Poincaré section from 1 to 14 (with some accepted small level of errors). When the periodicity is detected, the corresponding pixel in the chart is indicated by some color depending on the period, and the procedure goes to analyze the next point in the parameter plane. As the initial conditions at the new point it is reasonable to assign the state resulting in the end of iterations in the previous point ("scanning with inheritance") to accelerate the convergence to the steady state dynamics.
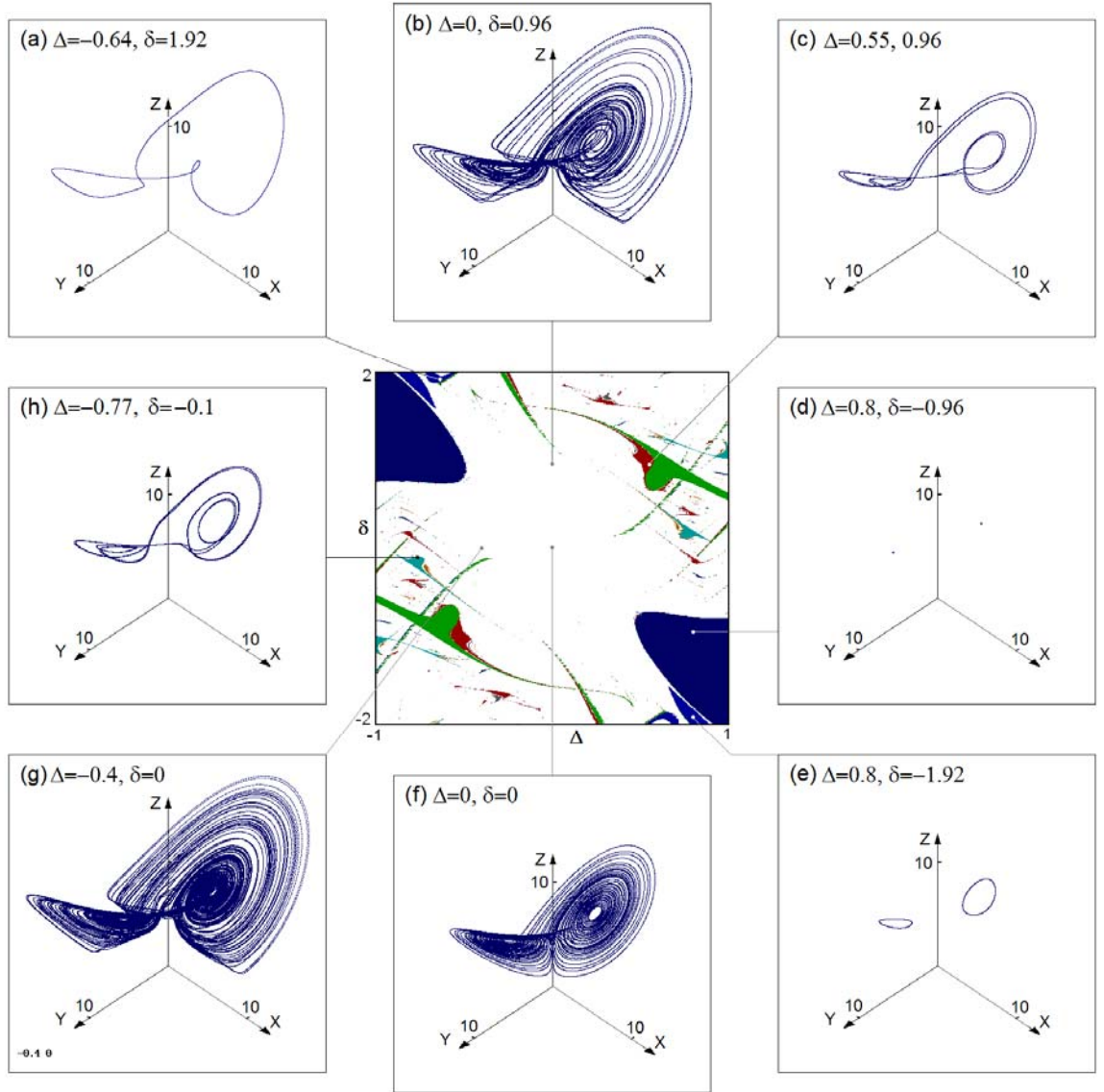
Figure 8: A chart of the system (17) in the plane of parameters Δ and δ and portraits of attractors corresponding to representative points of the parameter plane. Other parameters: $h = 5.962$, $\nu_1 = 1$, $\nu_2 = 4$.

In the center of Figure 8 the parameter plane chart is shown for the system (17), and on the periphery the portraits of attractors are depicted corresponding to some representative points of the parameter plane (Δ, δ). Attractors in panels (a), (c), (h), (e) to are limit cycles, i.e. periodic modes for oscillations of amplitudes in the colored parameter plane areas. On the other hand, attractors in the diagrams (b), (g), (f) are chaotic corresponding to not colored regions where the periodicity is not detected. Diagram (f) relates to the origin on the chart where the Lorenz type attractor occurs, which was discussed in the previous section. Dark blue areas in "north-west" and "south-east" parts of the chart correspond to the fixed point attractor of the Poincaré map (panel (e)) associated with a stable regime of stationary oscillations of constant amplitude in the initial equations.

Similar regimes are observed in numerical simulations of the original system of Kirchhoff's equations (7). Figure 9 shows attractors related to the system with the pump at an amplitude of 62.25 mV, and the resistances R_1=1 MΩ, R_2=250 kΩ, R_3=1 MΩ. The frequency of the pump and inductance L_3 were selected to provide the parameters Δ and δ indicated in the inscriptions, and the other parameter values correspond to the caption of Fig.2. The pictures clearly resemble those on the periphery of Fig. 8 with the difference that the trajectories on the attractors look a little "fluffed", which is obviously connected

10

with the presence of non-resonant components of relatively low amplitude contributing to the instantaneous values of dynamic variables, which were excluded in the amplitude equations. [2]
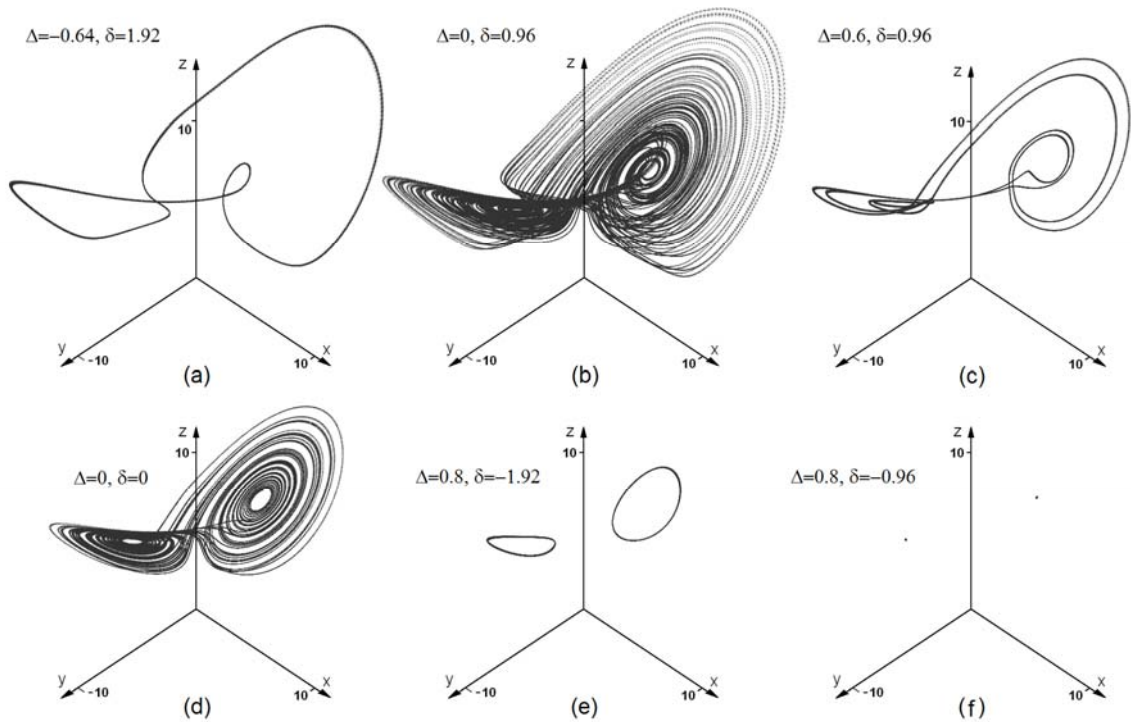

Figure 9: Portraits of attractors of the original Kirchhoff's equations (3) at the resistances R_1=1 MΩ, R_2=250 kΩ, R_3=1 MΩ and the pumping amplitude 62.25 mV. The pump frequency and the inductance L_3 were set to provide the parameter values Δ and δ: -0.64, 1.92 (a); 0, 0.96 (b); 0.6, 0.96 (c); 0,0 (d); 0.8, -1.92 (e); 0.8, -0.96 (f). The remaining parameters correspond to the caption of Fig.2.

Conclusion

We present analysis of the chaotic parametric oscillator based on three resonant circuits with pumping provided by periodic variation in voltage on a quadratic nonlinear element. It appears that the methodological value of the model is that it allows pure realization and exploration for the mechanism of parametric generation of chaos when two modes are excited due to the pump at the sum frequency, and the energy extraction is carried out by the mode at the difference frequency. This circuit may serve as an analog simulator for systems of different nature where the same mechanism of parametric oscillations take place, or, more widely, for systems where similar equations occur on some reason [42, 43].

If the case of deviation from the exact parametric resonance, instead of the quasi-hyperbolic Lorenz type attractor one obtains the dynamics although resembling those of Lorenz, but lacking robustness: by varying parameters destruction of chaos appears to be possible with the emergence of regular motions. This conclusion has been illustrated particularly by the chart of the plane of the detuning frequency parameters, which gives a visual representation of location of areas of chaotic and regular dynamics.

---

[2] The lack of a perfect match in the parameters with Fig.8 is due to the approximate nature of description in terms of slow amplitudes.

References

[1]   Vyshkind, S.Ya., Rabinovich, M.I. The phase stochastization mechanism and the structure of wave turbulence in dissipative media. JETP. Vol. 44 (2). P. 292-299.

[2]   Pikovski, A.S., Rabinovich, M.I., Trakhtengerts, V.Y. Appearance of chaos at decay saturation of parametric instability. JETP. 1978. Vol. 47. P. 715-719.

[3]   Rabinovich, M.I., Fabrikant, A.L. Stochastic wave self-modulation in nonequilibrium media. Sov. Phys. JETP. 1979. Vol. 50 (2). P. 311-317.

[4]   Louisell, W.H. Coupled Mode and Parametric Electronics. Wiley: New York, 1960. 268 p.

[5]   Akhmanov, S.A., Khokhlov, R.V. Parametric amplifiers and generators of light //Physics-Uspekhi. 1966. Vol. 9. No 2. P. 210-222.

[6]   Ostrovskii, L.A., Papilova, I.A., Sutin, A.M. Parametric Ultrasound Generator. Soviet Journal of Experimental and Theoretical Physics Letters. 1972. Vol. 15. P. 322-323.

[7]   Akulenko, L.D. Parametric control of the oscillations and rotations of a physical pendulum (swing). Prikladnaya Matematika i Mekhanika, vol. 57, no. 2, p. 82-91.

[8]   Lorenz, E.N. Deterministic nonperiodic flow. Journal of the Atmospheric Sciences. 1963. Vol. 20. No 2. P. 130-141.

[9]   Sparrow, C. The Lorenz Equations: Bifurcations, Chaos, and Strange Attractors. NY, Heidelberg, Berlin: Springer-Verlag, 1982. 270 p.

[10]   Kuznetsov, S. P. Dynamic Chaos. 2nd ed. Fizmatlit: Moscow, 2006. 356 p.

[11]   Anishchenko, V.S. Attractors of Dynamical Systems. Izvestija VUZ. Applied Nonlinear Dynamics. 1997. Vol. 5. No 1. P. 109-127.

[12]   Bonatti, C., Diaz, L.J., Viana, M. Dynamics Beyond Uniform Hyperbolicity. A Global Geometric and Probobalistic Perspective. Encyclopedia of Mathematical Sciences. Vol.102. Springer: Berlin, Heidelberg, New-York, 2005. 384 p.

[13]   Banerjee, S., Yorke, J.A., Grebogi, C. Robust chaos. Phys. Rev. Lett. 1998. Vol. 80. P. 3049-3052.

[14]   Elhadj, Z. and Sprott, J.C. Robust Chaos and its Applications. Singapore: World Scientific, 2011. 454 p.

[15]   Oraevskiĭ A. N. Masers, lasers, and strange attractors. Quantum Electronics. 1981. Vol. 11. No 1. P. 71-78.

[16]   Oraevsky, A. N. Dynamics of single-mode lasers and dynamical chaos. Izvestija VUZ. Applied Nonlinear Dynamics. 1996. Vol. 4, No 1. P. 3-13.

[17]   Haken, H. Analogy between higher instabilities in fluids and lasers. Physics Letters A. 1975. Vol. 53. No 1. P. 77-78.

[18]   Kolář, M., Gumbs, G. Theory for the experimental observation of chaos in a rotating waterwheel. Physical Review A. 1992. Vol. 45. No 2. P. 626-637.

[19]   Glukhovskii, A.B. Nonlinear systems that are superpositions of gyrostats. Soviet Physics Doklady. 1982. Vol. 27. P. 823.

[20]   Doroshin, A.V. Modeling of chaotic motion of gyrostats in resistant environment on the base of dynamical systems with strange attractors.Communications in Nonlinear Science and Numerical Simulation. 2011. Vol. 16. No 8. P. 3188-3202.

[21]   Chen, H.K., Lee, C.I. Anti-control of chaos in rigid body motion. Chaos, Solitons & Fractals. 2004. Vol. 21. No 4. P. 957-965.

[22]   Poland, D. Cooperative catalysis and chemical chaos: a chemical model for the Lorenz equations. Physica D. 1993. Vol. 65. No 1. P. 86-99.

[23]   Cuomo, K.M., Oppenheim, A.V. Circuit implementation of synchronized chaos with applications to communications. Phys. Rev. Lett. 1993. Vol. 71. No 1. P. 65-68.

[24] Peters, F., Lobry, L., Lemaire, E. Experimental observation of Lorenz chaos in the Quincke rotor dynamics. Chaos: An Interdisciplinary Journal of Nonlinear Science. 2005. Vol. 15. No 1. P. 013102.

[25] Rucklidge, A. M. Chaos in magnetoconvection. Nonlinearity. 1994. Vol. 7. No 6. P. 1565-1591.

[26] Hemail, N. Strange attractors in brushless DC motor. IEEE Transactions on Circuits and System-I. 1994. Vol. 41. No 1. P. 40-45.

[27] Gibbon, J. D., McGuinness, M. J. The real and complex Lorenz equations in rotating fluids and lasers. Physica D: Nonlinear Phenomena. 1982. Vol. 5. No 1. P. 108-122.

[28] Fowler, A. C., Gibbon, J. D., McGuinness, M. J. The complex Lorenz equations. Physica D: Nonlinear Phenomena. 1982. Vol. 4. No 2. P. 139-163.

[29] Mahmoud, G. M., Ahmed, M. E., Mahmoud, E. E. Analysis of hyperchaotic complex Lorenz systems. International Journal of Modern Physics C. 2008. Vol. 19. No 10. P. 1477-1494.

[30] Wang, P. K. C., Masui, K. Intermittent phase unlocking in a resonant three-wave interaction with parametric excitation. Physics Letters A. 1981. Vol. 81. No 2. P. 97-101.

[31] Letellier, C., Aguirre, L.A., Maquet, J., Lefebvre, B. Analogy between a 10D model for nonlinear wave–wave interaction in a plasma and the 3D Lorenz dynamics. Physica D: Nonlinear Phenomena. 2003. Vol. 179. No 1. P. 33-52.

[32] Llibre, J., Messias, M., da Silva, P. R. On the global dynamics of the Rabinovich system. Journal of Physics A: Mathematical and Theoretical. 2008. Vol. 41. No 27. P. 275210.

[33] Kuznetsov, S.P. Parametric chaos generator operating on a varactor diode with the instability limitation decay mechanism. Technical Physics, **61**, 2016, No. 3, 436–445.

[34] Liu, Y., Yang, Q., Pang, G. A hyperchaotic system from the Rabinovich system. Journal of Computational and Applied Mathematics. 2010. Vol. 234. No 1. P. 101-113.

[35] Kuznetsov, S.P. Dynamical chaos and uniformly hyperbolic attractors: from mathematics to physics. Physics-Uspekhi. 2011. Vol. 54. No 2. P. 119-144.

[36] Tucker, W. A rigorous ODE solver and Smale's 14th problem. Comp. Math. 2002. Vol. 2. P. 53–117.

[37] Benettin, G., Galgani, L., Giorgilli, A., Strelcyn, J.-M. Lyapunov characteristic exponents for smooth dynamical systems and for Hamiltonian systems: A method for computing all of them. Meccanica. 1980. Vol. 15. P. 9-20.

[38] Hénon, M. A two-dimensional mapping with a strange attractor. Commun. Math. Phys. 1976. Vol. 50. P. 69–77.

[39] Rössler, O.E. Continuous chaos: four prototype equations. Ann. New York Academy of Sciences. 1979. Vol. 316. P. 376-392.

[40] Afraimovich, V.S. Strange attractors and quasiattractors. Nonlinear and turbulent processes in physics. 1984. Vol. 1. P. 1133-1138.

[41] Shilnikov, L.P. Bifurcations and strange attractors. Vestnik Nizhegorodskogo Universiteta. 2011. No. 4 (2). P. 364-366.

[42] Kozlov, V.V. On the problem of fall of a rigid body in a resisting medium. Moscow University Mechanics Bulletin. 1990. Vol. 45. No 1. P. 30-35.

[43] Kuznetsov, S. P. Plate falling in a fluid: Regular and chaotic dynamics of finite-dimensional models. Regular and Chaotic Dynamics. 2015. Vol. 20. No 3. P. 345-382.